Co-Ex: A Torque-*Co*ntrollable Lower Body *Ex*oskeleton for Dependable Human-Robot *Co-ex*istence

Mehmet C. Yildirim, Ahmet Talha Kansizoglu, Sinan Emre, Mustafa Derman, Sinan Coruk, Ahmed Fahmy Soliman, Polat Sendur, Barkan Ugurlu

***Abstract*— In this paper, we present our research study concerning the design and development of an exoskeleton that aims to provide 3D walking support with minimum number of actuators. Following a prior simulation study, the joint configuration was primarily determined. In order for the exoskeleton to possess advanced characteristics, the following design criteria were investigated: i) all the actuators (hip/knee/ankle) were deployed around the waist area to decrease leg weight and improve wearability, ii) custom-built series elastic actuators were used to power system for high fidelity torque-controllability, iii) 3D walking support is potentially enabled with reduced power requirements. As a result, we built the first actual prototype to experimentally verify the aforementioned design specifications. Furthermore, the preliminary torque control experiments indicated the viability of torque control.**

I. Introduction

Paraplegia is a particular type of disease that affects the lower extremity motor and sensory functions. To provide mobility for people with paraplegia, low cost and practical systems, e.g., wheelchairs, can be utilized. However, solutions as mentioned earlier become ineffective on uneven or inclined terrains and may also cause pressure sores due to long term usage [1], [2]. In this regard, wearable exoskeletons can be a more favorable solution owing to their walking support abilities that enable improved neuroplasticity [3].

Most state-of-the-art lower body exoskeletons possess 2 active Degrees of Freedom (DOFs) along the Flexion/Extension (F/E) axis through the knee and hip joints [4]–[6]. Such a kinematic configuration is designed with the intention of moving the user's leg forward with the least number of actuators. While this strategy may minimize cost, weight and energy requirements, it enforces the user to actively engage its upper body via crutches to maintain static balance.

Indeed, the aforementioned 2 active DoF per leg exoskeletons demonstrated successful walking support for human users; yet, the long term use of such devices is argued to be questionable due to limited gait capability and extensive upper body effort [7]–[9]. These problems may be prevented with the expense of increased active DoFs. For instance, Ugurlu et al. developed an exoskeleton via the addition of an active ankle joint along D/PF (Dorsi/Plantar Flexion) to address self-balancing capability in the sagittal plane [10]. For the Mindwalker exoskeleton, the researchers further added an active joint along the hip A/A (Adduction/Abduction) joint to enable CoM (Center of Mass) shift [11]. Further efforts on this matter led to fully actuated exoskeletons with 6 active DoFs per leg [12], [13].

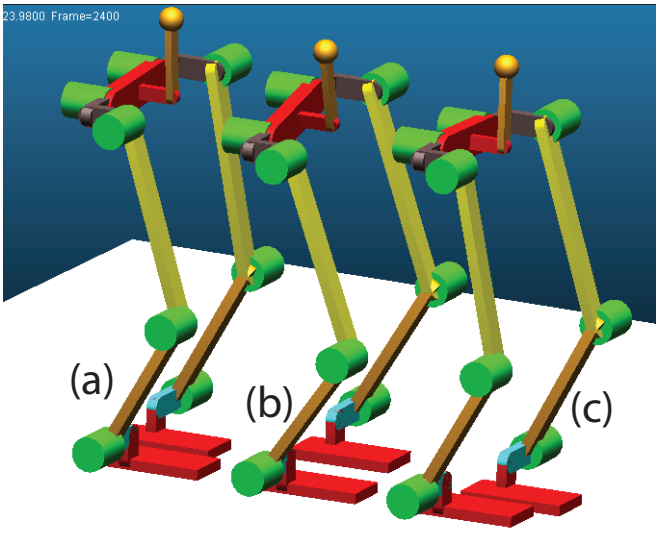

Fig. 1. A single step from our simulation studies [14]: a) double support support phase, b) single support phase (left foot swings), c) swinging left foot lands.

Obviously, increasing the number of active joints paves the way for improved walking gait support; however, the long term use of exoskeletons dictates reduced power consumption and light mechanical design requirements. In other words, there are contradictory requirements for the enhanced gait capability objective. With this trade-off in mind, we ran simulation studies in MSC ADAMS environment [14] to determine the minimum number of active joints to ensure 3-D walking while considering gait determinants [15]. Three snapshots from the simulation experiment are displayed in Fig. 1. As a result, we observed that 3D walking could be achieved via 4 active joints per leg configuration, namely, a 2 DoF hip joint along the F/E and A/A axes, a 1 DoF knee joint along the F/E axis, and a 1 DoF ankle joint along the D/PF joint; see Fig. 2.

Considering the findings discussed above, the main research study in this paper is the mechatronics hardware design and development for an exoskeleton system, namely CoEx, with the following advanced properties : i) all the

The authors are with the Dept. of Mechanical Engineering, Ozyegin University, 34794 Istanbul, Turkey. e-mail: {barkan.ugurlu, polat.sendur}@ozyegin.edu.tr e-mail: {mehmet.yildirim, talha.kansizoglu, fahmy.ahmed, sinan.emre, mustafa.derman, sinan.coruk}@ozu.edu.tr

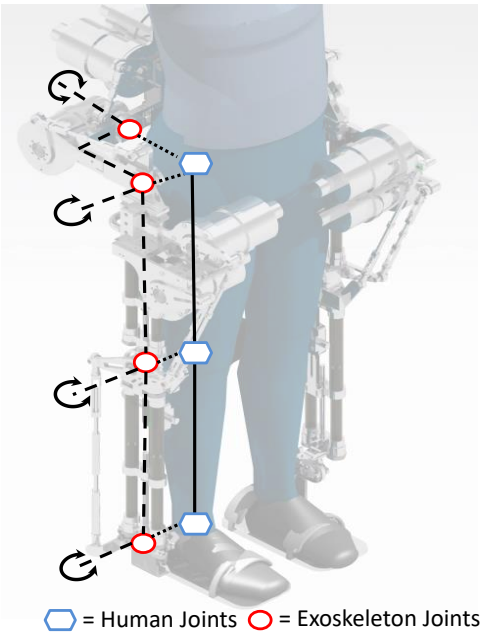

Fig. 2. Joint configuration of the exoskeleton, displayed only for a single leg. Note that actuator axes do not directly indicate the joint axes; see Fig. 3. A simplified human leg kinematics is considered.

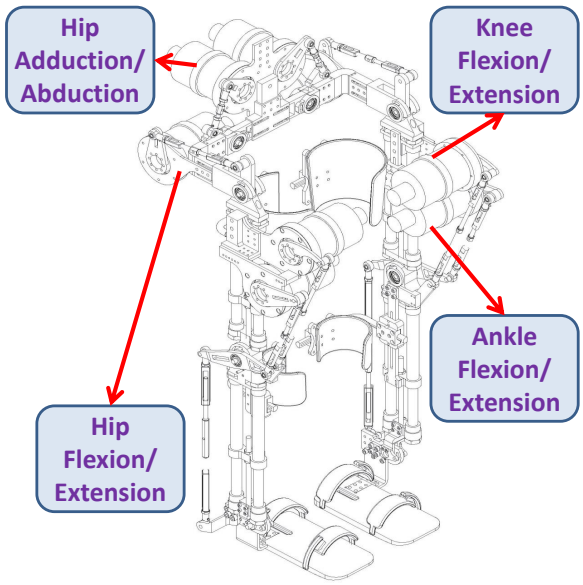

Fig. 3. CAD structure of the CoEx exoskeleton as the position of the actuators highlighted. Various four-bar mechanisms are utilized to transmit power from motors which are deployed around the waist area.

actuators are deployed around the waist area to enhance inverted pendulum analogy and to decrease leg weights for enhanced wearability, ii) long term 3D walking support is potentially enabled with the least number of actuators for reduced power requirements, iii) torque control is made possible with the help of stand-alone SEA (Series Elastic Actuator) units with high torque-to-weight ratio and high torque resolution. Developing such an exoskeleton prototype enables us to investigate whether these advanced properties can be satisfied with the proposed system, and if not, it would lead us to further improvements to pursue these design objectives.

The remainder of this paper is organized as follows, In Section II, the development of mechatronics hardware is explained in details with a particular emphasis on SEA units, mechanical structure, manufacturing process, electronics design, and user safety. Section III presents preliminary torque control experiments. Finally, the paper is concluded in Section V.

II. Mechatronics Hardware Development

A. Leg Design Approach

Due to multi-dimensionality, discontinuous contacts, and uncertainties associated with the exact dynamic models of legged robots, researchers often prefer reduced-order abstracted models that encapsulate the dominant characteristics of the system. In these models, the whole body is represented as a single body that is attached to the ground via a massless telescopic leg [16]. Therefore, if the real physical system mass is accumulated around the upper torso, these approximations can represent the dynamic system behavior more accurately compared to models with distributed mass [17]. In recently developed systems were adopted this pendulum-like structure by taking the knee (F/E) actuator to hip level and the toe (ankle) joint actuator to knee level, and connecting all these transferred actuators with a four-bar-linkage [18]. This actuator design is also implemented in other systems to reduce leg inertia [19].

We believe that we can make use of such a strategy in exoskeleton actuation as well. With this in mind, we followed a design approach in which all the actuators, even including ankle actuators, are deployed around the waist area; see Fig. 3 for the overall CAD of the robot and Fig. 4 for the manufactured exoskeleton. The remainder subsection discloses the design blocks we bring together to realize the CoEx hardware.

B. SEA-Powered Joint Units

Torque control and physical elasticity properties are crucial in systems like exoskeleton robots, where a robot and a human work within a physical contact [20]. Controlled elasticity plays an important role when compensating the reaction forces from the ground [4]. Importance of the torque-controlled actuators become prominent by its straight forward relation to torque control, which strengthens the interaction competence [21].

Even though all previous SEAs showed sufficient performance, a new SEA which capable of actuating the proposed exoskeleton was required. The CAD model of the developed SEA; CoEx-SEA-B is displayed in Fig. 5. A custom made torsional spring was designed to and connected to the output of the gearbox (Harmonic Drive CPL-25A-100-2A2). The output cap of the SEA unit is attached to the outer circle of the spring. Two 23-Bit (Broadcom Avago

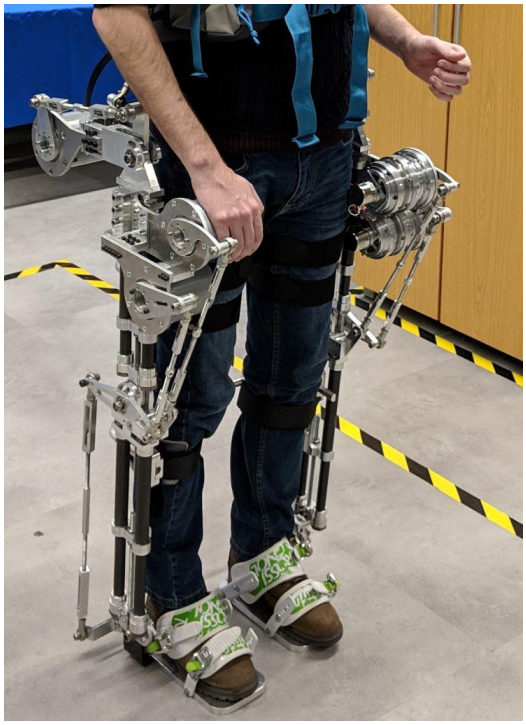

Fig. 4. Manufactured exoskeleton system, worn by a male able-bodied.

AS38 H39ES135) encoders are integrated to measure the motor angle and torsional deflection (on the link side), respectively. Advantages of encoder-based system' torque-control capacity against load-cell integrated systems have been highlighted in the literature [22].By considering the weight Frameless Brushless DC Motors (Kollmorgen TBM-7615) were integrated, due to their easy to customize nature. For further details, see [23].

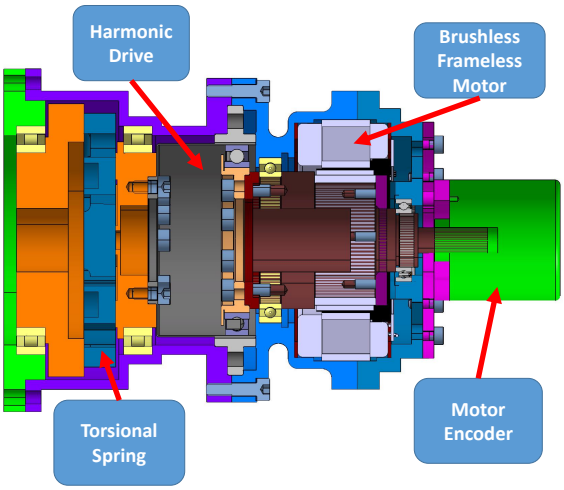

Fig. 5. CoEx-SEA-B unit CAD section view

TABLE I
SEA MODULE PROPERTIES

Specification	CoEx-SEA (B)
Max. Angular Speed (rpm)	44.09
Max. Continuous Torque (Nm)	96
Mass (kg)	2.45
Dimensions (r x L) (mm x mm)	50 x 175
Stiffness (Nm/deg)	45.5
Torque Resolution (mNm)	7.8
Torque-to-mass Ratio (Nm/kg)	39.2
Cost (Euro)	$\approx$ 3100

C. Exoskeleton Design

The design requirements related to reaction forces and torque requirements from the current literature were investigated. However, minimal information was found on such design requirements. Therefore, design requirements were investigated with the aid of numerical simulations. Towards that goal, an integrated human and exoskeleton model was co-simulated using MATLAB and MSC.Adams. Details of the simulation model can be found in [24]. A human, with the height and weight of $190cm$ and $90kg$, respectively, was placed with an exoskeleton concept which was created using CAD software. The model is simulated under harmonic excitation with 1.5 Hz, which corresponds to the half of human gait frequency ($\approx 1.5Hz$) Thus, the maximum velocities at the joints have been set to $9.55rad/s$. Finally, the maximum joints forces were identified from the numerical integration.

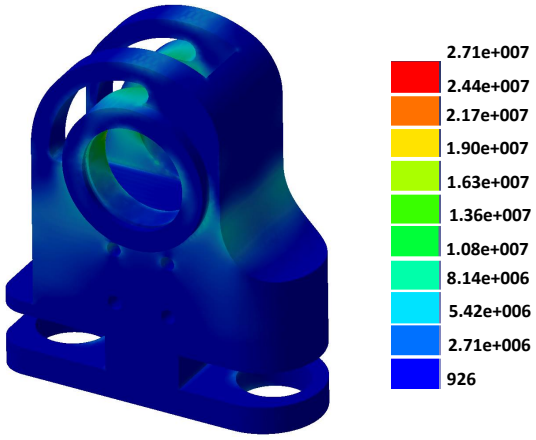

Fig. 6. FEA result of the exoskeleton knee joint

In the joint design process, the most vulnerable joint of the robot was used as the selection criterion for the motion components (bearings, shafts, bushings). The worst possible scenario for each joint was calculated using the transverse and frontal axis values, see Fig. 6 for the effects of the loading on a joint. By considering the maintenance, the bearing selection is made in accordance with the most critical joint was made. The same bearing is also used for all other joints. In this study, approximate maintenance life for the design was chosen as one year. However, considering the fact that possible daily usage of a regular user is less than 24 hours per day, it is likely that the actual life of the bearing is

much longer than one year. Load rating (C_{10}) of the desired bearing was calculated for this given lifetime and maximum possible load value with a stochastic safety factor of 1.5.

The adjustable limb was an essential feature of the design to consider. Thus, the literature has been reviewed to determine the required limb dimensions, especially, for the thigh and the shank [25]. A range of different link lengths were set in accordance with these collected values as; Thigh $459mm-316mm$ and Shank $473mm-373mm$. Bartenbach et al. suggested a two hollow carbon-fibre centred design in [26]. In this design, designers considered adjustability of the different links of the robot with respect to the size of the human limbs. Additionally, it was observed that designers used similar joint structures for each link. Even though this strategy creates many advantages, especially for manufacturing and maintenance, since each joint has unique needs, such a strategy can lead to overly safe designs. Hence, by considering features like adjustability, joint sequence, and manufacturability, two tube design without the further joint design was selected for the base of our lower body exoskeleton.

Inverted pendulum structure of the exoskeleton caused a challenge, in the transmission of the power from the actuator to its related joint. Rigidity must be the key component at this point since the designed system leans on the elastic actuators power transmission with relatively soft power transmitters like belts and chains could eventually affect the compliance of the system. Because of these reasons, already suggested [27], [28] structures were not preferred. However, robots and exoskeletons use rigid four-bar and five-bar mechanisms to transfer motion [18], [19], [29]. By considering these aforementioned linkage structures power transmission of the joints was done through four-bar mechanisms.

It is also an important design consideration to make sure that there a firm grip between the robot and human since the user has lower body paralysis. There is a vast body of exoskeleton design in the literature with such design attribute [10], [27], [30]. In general, orthosis molds are made of polyethylene, polypropylene, and polycarbonate. Due to their flexibility, plastic and its derivatives are the most preferred materials for that kind of equipment. However, polyethylene orthosis attachments were chosen in this study considering better durability performance.

D. Manufacturing Process

The manufacturing process of the exoskeleton can be divided into two distinct sections. The initial section includes the manufacturing of the motor casings, foot plates, size adjusters of the hip section, joint shafts and other auxiliary support structures. These parts are manufactured using three main manufacturing techniques: **i)** turning, **ii)** milling, and **iii)** laser cut. Aluminium 6000 series is used for the aforementioned parts except for the joint shafts, which were manufactured from stainless steel.

The later section is realized via adhesion. The carbon-fibre telescopic leg structures are fused using adhesives into the aluminium connector caps, which maintains the connection of the legs with the rest of the system and act as a lock for the size adjustable leg structures.

E. Electronics Design

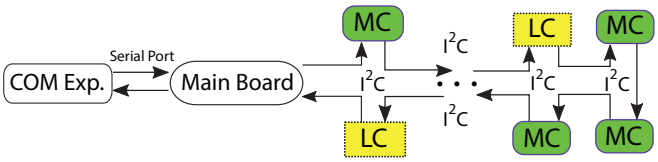

Fig. 7. Electronic hardware implementation with the communication structure

Electronic implementation of the exoskeleton consists of various modules based on STM32 microcontrollers. These modules are the main board, motor control (MC) boards, and load cell (LC) boards respectively, see Fig. 8. The main board communicates with the MC and LC via I^2C standard. This connection was designed with a loop as shown in Fig. 7. MC board has a PWM output pin to send commands to the motor driver, a digital pin to enable and disable the motor and two encoder inputs to measure the motor position and the deflection. The LC board amplifies the analog output of the load cells and converts the analog signal into digital data. COM Express is the main computation unit of the exoskeleton and the communication with the main board is serial communication.

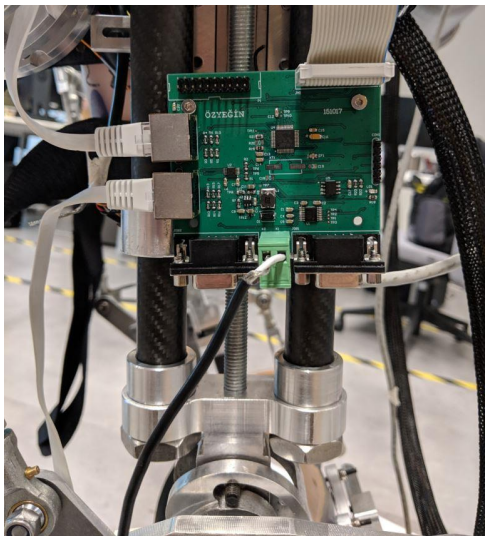

Fig. 8. Integrated electronic board on left thigh link

F. Safety

Considering that safety is one of the most important design considerations in the exoskeleton development, a three-layered safety protocol including mechanical, electrical and software, suggested by Otten et al. has been implemented [31]. As part of the mechanical safety layer, each joint of the CoEx is limited to a level, lower than the human joint range, as mentioned in [23]. Besides, the thermal structure of the SEAs is evaluated against the potential burn hazard. Finally,

it is ensured that the parts in motion (four-bar' crank and rocker parts, joint shafts) are widely spaced such that they do not cause harm to the user.

As the second layer of the safety precautions, electronic boards were designed to be connected as a loop. Onboard LEDs are programmed to blink in case of any connection setbacks between the boards. If the slave boards cannot deliver the requested data, e.g. encoder position, or if it fails to perform the required action e.g, enabling the motor, an error code is sent to the main board. Based on the error code, the program is expected to disable the motor via a digital signal. In addition to the mechanical and electrical safety measures, a software-based motor emergency algorithm was implemented in order to take account the instability of the exoskeleton. If the motor command signal is at maximum for a finite amount of cycles, the emergency counter is incremented by one until it reaches the safety limit. If the safety limit is exceeded, the motor is disabled until the program is reset.

III. Preliminary Experiments: Torque Control

To demonstrate the torque control performance of the SEAs, results from preliminary experiments are presented in this section. Experiment results were conducted on a single joint system controlled via a Cascaded PID controller proposed in [32]. While the outer loop performs the torque control of the actuator with a PID controller, the inner loop achieves the velocity control of the motor side with a PI controller. In other words, the outer loop generates a motor velocity reference for the inner loop. The controller configuration can be seen in Fig. 9 where K is the spring constant, τ_d and τ_m are the output torque of the actuator and motor torque, θ_d and $\dot{\theta}_m$ are the deflection and motor velocity respectively. T_d is the time constant for the low-pass filter and ^{ref} indicates the reference value.

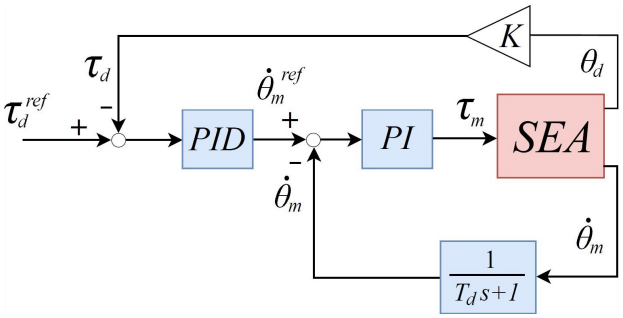

Fig. 9. Cascaded PID controller block diagram

Tuning of the Cascaded PID controller was achieved intuitively with respect to stability criteria defined in [32]. Controller parameters can be seen in Table II where $_1$ stands for PID and $_2$ stands for PI controller. Sinusoidal tracking performance of the controller can be seen in Fig. 10. Tracking and RMS errors were given for three frequencies that are 3, 6 and 12 rad/s. The controller bandwidth was calculated as 17 Hz.

TABLE II
Cascaded PID Controller Parameters

Parameters	***Explanation***	***Value***
–	Sampling rate	2 kHz
K_{p1}	Outer loop proportional gain	16
K_{i1}	Outer loop integral gain	7
K_{d1}	Outer loop derivative gain	0.8
K_{p2}	Inner loop proportional gain	0.045
K_{i2}	Inner loop integral gain	0.012
T_d	LPF time constant	0.00167

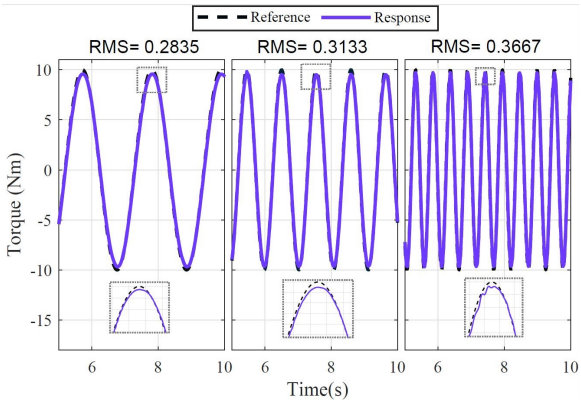

Fig. 10. Sinusoidal tracking with frequencies of 3, 6, and 12 rad/s

IV. Discussion

In this paper a new lower body exoskeleton design is presented, as every new design has its own, this new design does bring some further questions too. A few selected question can be named here with our perspective on these topics; the higher center of the mass structure is a common property in many of the humanoids, which does not cause stabilization problem, with the same characteristic we expect a stabilized walking quality. As different than the other exoskeleton designs more weight is carried on the level of the upper leg and the hip, this may bring the question of the effects of the increasing joint load for the knees and etc.. However, as an exoskeleton designed specifically for the paraplegics, the exoskeleton does not reflect any load on the human counterpart. Finally, the apparent difference between the human musculoskeletal and the exoskeleton simplified the joint-link structure, this is a question require further attention and experimental data.

V. Conclusion

This paper presented our research for the mechatronics hardware realization of CoEx, an exoskeleton that can potentially provide 3D walking support with the least possible number of active joints. To improve wearability and achieve pendulum analogy, all the actuators are deployed around the waist area. Its joints are actuated via custom-built SEA units with a high torque-to-weight ratio. The preliminary experimental results indicate that torque-controllability is viable for the proposed exoskeleton system.

Currently, we are investigating feasible 3D walking experiments with the proposed exoskeleton system. Therefore, we

consider experimental verification as future work.

ACKNOWLEDGEMENTS

This work is supported by the Scientific and Technological Research Council of Turkey (TÜBİTAK), with the project 215E138. The authors thank U. Yildirim, O. Topcam, S. Hamza, O. Cetin, B. Sunal, M. Karaca, O. Ersoy, A. Yasar, M. Odabasi, E. T. Karasu, and I. N. Yildiz.

REFERENCES

[1] A. Kittel, A. D. Marco, and H. Stewart, "Factors influencing the decision to abandon manual wheelchairs for three individuals with a spinal cord injury," *Disability and Rehabilitation*, vol. 24, no. 1-3, pp. 106–114, 2002.

[2] T. Sumiya, K. Kawamura, A. Tokuhiro, H. Takechi, and H. Ogata, "A survey of wheelchair use by paraplegic individuals in japan. part 2: prevalence of pressure sores," *Spinal cord*, vol. 35, no. 9, p. 595, 1997.

[3] J. V. Lynskey, A. Belanger, and R. Jung, "Activity-dependent plasticity in spinal cord injury," *Journal of rehabilitation research and development*, vol. 45, no. 2, p. 229, 2008.

[4] B. Ugurlu, H. Oshima, and T. Narikiyo, "Lower body exoskeleton-supported compliant bipedal walking for paraplegics: How to reduce upper body effort?" in *Robotics and Automation (ICRA), 2014 IEEE International Conference on*. IEEE, 2014, pp. 1354–1360.

[5] L. Brenner, "Exploring the psychosocial impact of ekso bionics technology," *Archives of Physical Medicine and Rehabilitation*, vol. 97, no. 10, p. e113, 2016.

[6] K. A. Strausser, T. A. Swift, A. B. Zoss, H. Kazerooni, and B. C. Bennett, "Mobile exoskeleton for spinal cord injury: Development and testing," in *ASME 2011 Dynamic Systems and Control Conference and Bath/ASME Symposium on Fluid Power and Motion Control*. American Society of Mechanical Engineers, 2011, pp. 419–425.

[7] V. Lajeunesse, C. Vincent, F. Routhier, E. Careau, and F. Michaud, "Exoskeletons' design and usefulness evidence according to a systematic review of lower limb exoskeletons used for functional mobility by people with spinal cord injury," *Disability and Rehabilitation: Assistive Technology*, vol. 11, no. 7, pp. 535–547, 2016.

[8] I. Benson, K. Hart, D. Tussler, and J. J. van Middendorp, "Exoskeletons' design and usefulness evidence according to a systematic review of lower limb exoskeletons used for functional mobility by people with spinal cord injury," *Clinical Rehabilitation*, vol. 30, no. 1, pp. 73–84, 2016.

[9] A. E. Palermo, J. L. Maher, C. B. Baunsgaard, and M. S. Mash, "Clinician-focused overview of bionic exoskeleton use after spinal cord injury," *Topics in Spinal Cord Injury Rehabilitation*, vol. 23, no. 3, pp. 234–244, 2017.

[10] B. Ugurlu, C. Doppmann, M. Hamaya, P. Forni, T. Teramae, T. Noda, and J. Morimoto, "Variable ankle stiffness improves balance control: Experiments on a bipedal exoskeleton," *IEEE/ASME Transactions on Mechatronics*, vol. 21, no. 1, pp. 79–87, 2016.

[11] S. Wang, L. Wang, C. Meijneke, E. van Asseldonk, T. Hoellinger, G. Cheron, Y. Ivanenko, V. L. Scaleia, F. Sylos-Labini, M. Molinari, F. Tamburella, F. T. I. Pisotta, M. Ilkovitz, J. Gancet, Y. Nevatia, R. Hauffe, F. Zanow, and H. van der Kooij, "Design and control of the mindwalker exoskeleton," *IEEE Transactions on Neural Systems and Rehabilitation Engineering*, vol. 23, no. 2, pp. 277–286, 2015.

[12] A. Agrawal, O. Harib, A. Hereid, S. Finet, M. Masselin, L. Praly, A. D. Ames, K. Sreenath, and J. W. Grizzle, "First steps towards translating hzd control of bipedal robots to decentralized control of exoskeletons," *IEEE Access*, vol. 5, pp. 9919–9934, 2017.

[13] G. Barbareschi, R. Richards, M. Thornton, T. Carlson, and C. Holloway, "Statically vs dynamically balanced gait: Analysis of a robotic exoskeleton compared with a human," in *Engineering in Medicine and Biology Society (EMBC), 2015 37th Annual International Conference of the IEEE*. IEEE, 2015, pp. 6728–6731.

[14] A. F. Soliman, P. Sendur, and B. Ugurlu, "3-d dynamic walking trajectory generation for a bipedal exoskeleton with underactuated legs: A proof of concept," in *IEEE International Conference on Rehabilitation Robotics (ICORR) 2019*, Submitted.

[15] A. D. Kuo, "The six determinants of gait and the inverted pendulum analogy: A dynamic walking perspective," *Human Movement Science*, vol. 26, no. 4, pp. 617–656, 2007.

[16] S. Kajita, F. Kanehiro, K. Kaneko, K. Yokoi, and H. Hirukawa, "The 3d linear inverted pendulum mode: A simple modeling for a biped walking pattern generation," in *Intelligent Robots and Systems, 2001. Proceedings. 2001 IEEE/RSJ International Conference on*, vol. 1. IEEE, 2001, pp. 239–246.

[17] X. Da, O. Harib, R. Hartley, B. Griffin, and J. W. Grizzle, "From 2d design of underactuated bipedal gaits to 3d implementation: Walking with speed tracking," *IEEE Access*, vol. 4, pp. 3469–3478, 2016.

[18] Z. Xie, G. Berseth, P. Clary, J. Hurst, and M. van de Panne, "Feedback control for cassie with deep reinforcement learning," in *Intelligent Robots and Systems, 2007. IEEE/RSJ International Conference on*, 2018, pp. 1–6.

[19] N. Tsagarakis, F. Negrello, M. Garabini, W. Choi, L. Baccelliere, V. Loc, J. Noorden, M. Catalano, M. Ferrati, L. Muratore *et al.*, "Walkman humanoid platform," in *The DARPA Robotics Challenge Finals: Humanoid Robots To The Rescue*. Springer, 2018, pp. 495–548.

[20] A. De Santis, B. Siciliano, A. De Luca, and A. Bicchi, "An atlas of physical human–robot interaction," *Mechanism and Machine Theory*, vol. 43, no. 3, pp. 253–270, 2008.

[21] C. Lagoda, A. C. Schouten, A. H. A. Stienen, E. E. G. Hekman, and H. van der Kooij, "Design of an electric series elastic actuated joint for robotic gait rehabilitation training," in *2010 3rd IEEE RAS EMBS International Conference on Biomedical Robotics and Biomechatronics*, Sept 2010, pp. 21–26.

[22] N. Kashiri, J. Malzahn, and N. G. Tsagarakis, "On the sensor design of torque controlled actuators: A comparison study of strain gauge and encoder-based principles," *IEEE Robotics and Automation Letters*, vol. 2, no. 2, pp. 1186–1194, 2017.

[23] M. C. Yildirim, A. T. Kansizoglu, P. Sendur, and B. Ugurlu, "High power series elastic actuator development for torque-controlled exoskeletons," in *International Symposium on Wearable Robotics*, 2018, pp. 70–74.

[24] M. C. Yildirim, P. Sendur, A. F. Soliman, and B. Ugurlu, "Optimal stiffness tuning for a lower body exoskeleton with spring-supported passive joints," in *2018 7th IEEE International Conference on Biomedical Robotics and Biomechatronics (Biorob)*, Aug 2018, pp. 531–536.

[25] M. Hora, L. Soumar, H. Pontzer, and V. Sládek, "Body size and lower limb posture during walking in humans," *PloS one*, vol. 12, no. 2, p. e0172112, 2017.

[26] V. Bartenbach, M. Gort, and R. Riener, "Concept and design of a modular lower limb exoskeleton," in *in proc. of 2016 6th IEEE International Conference on Biomedical Robotics and Biomechatronics (BioRob)*. IEEE, 2016, pp. 649–654.

[27] T. Vouga, R. Baud, J. Fasola, M. Bouri, and H. Bleuler, "Twiice - a lightweight lower-limb exoskeleton for complete paraplegics," in *Rehabilitation Robotics (ICORR), 2017 International Conference on*. IEEE, 2017, pp. 1639–1645.

[28] Z. F. Lerner, D. L. Damiano, H.-S. Park, A. J. Gravunder, and T. C. Bulea, "A robotic exoskeleton for treatment of crouch gait in children with cerebral palsy: Design and initial application," *IEEE Transactions on Neural Systems and Rehabilitation Engineering*, vol. 25, no. 6, pp. 650–659, 2017.

[29] Y. Liao, Z. Zhou, and Q. Wang, "Biokex: A bionic knee exoskeleton with proxy-based sliding mode control," in *in proc. of 2015 IEEE International Conference on Industrial Technology (ICIT)*. IEEE, 2015, pp. 125–130.

[30] B. N. Fournier, E. D. Lemaire, A. J. Smith, and M. Doumit, "Modeling and simulation of a lower extremity powered exoskeleton," *IEEE Transactions on Neural Systems and Rehabilitation Engineering*, vol. 26, no. 8, pp. 1596–1603, 2018.

[31] A. Otten, C. Voort, A. Stienen, R. Aarts, E. van Asseldonk, and H. van der Kooij, "Limpact: A hydraulically powered self-aligning upper limb exoskeleton," *IEEE/ASME transactions on mechatronics*, vol. 20, no. 5, pp. 2285–2298, 2015.

[32] H. Vallery, R. Ekkelenkamp, H. Van Der Kooij, and M. Buss, "Passive and accurate torque control of series elastic actuators," in *Intelligent Robots and Systems, 2007. IROS 2007. IEEE/RSJ International Conference on*, 2007, pp. 3534–3538.